Theor Chem Acc (2011) 130:323–331
DOI 10.1007/s00214-011-0981-1

REGULAR ARTICLE

DFT and ONIOM study on the alkylation of the lithium enolate in solution: microsolvation cluster models for CH_2=CHOLi + CH_3Cl + $(THF)_{0–6}$

Kaori Ando · Keiji Morokuma

Received: 23 March 2011 / Accepted: 15 June 2011 / Published online: 29 June 2011

Abstract DFT computational study on the alkylation of the lithium enolate derived from acetaldehyde with MeCl was performed. The reaction of the free enolate CH_2=CHO^- with MeCl has an early transition state with low barrier, and the reaction of its lithium enolate gave a cyclic transition structure with high activation energy; neither of them is a good model for reaction in solution. In the presence of 1–6 THF molecule(s), a typical S_N2 transition structures were obtained with reasonable activation energies after the PCM correction. Especially, the reaction in the presence of three THF molecules completed the tetra-coordination of the lithium cation, and structurally and energetically, this is an optimal model for the reaction in the solution. The transition structures were also located at the ONIOM level (high = B3LYP/6–31(+)G*: low = RHF/3–21 G*). The results are favorably compared with the full DFT results.

Keywords DFT calculations · ONIOM study · Alkylation of lithium enolate · Solvent effect

1 Introduction

Alkylation of lithium enolates with alkyl halides is one of the most important carbon–carbon bond-forming reaction in chemistry ([1] and reference cited therein). Although, many lithium enolates have been known to exist primarily as tetrameric and dimeric aggregates and the lithium cations are solvated, oversimplified models such as solvent-separated free enolate ions have been employed until recently for the computational models, for example, see [2, 3]. The development of new methodologies for asymmetric alkylation and their practical utility in the synthesis of biologically active compounds is now the subject of intensive investigation. The interest in stereospecific synthesis raises the need to know the three-dimensional transition structures including solvation and aggregation, which control the stereochemistry of the reaction for a review [4, 5]. Streitwieser and Schleyer theoretically studied the effect of dimethyl ether solvation on aggregated forms of the lithium enolate of acetaldehyde $(CH_2\text{=CHO-Li})_n(Me_2O)_x$, $n = 1–4$, $x = 0–4$ [6]. They concluded that the cubic tetramer is stable because of the electrostatic stabilization of aggregation, but the monomeric species are important in the equilibrium because of their high solvation energies. Furthermore, Streitwieser and his coworkers studied the aggregation and reactivity of lithium enolates in tetrahydrofuran (THF) by using a combination of UV–vis spectroscopy and coupled ion-pair equilibria [7–16]. They

---

Dedicated to Professor Shigeru Nagase on the occasion of his 65th birthday and published as part of the Nagase Festschrift Issue.

Electronic supplementary material The online version of this article (doi:10.1007/s00214-011-0981-1) contains supplementary material, which is available to authorized users.

K. Ando (✉)
Department of Chemistry, Faculty of Engineering,
Gifu University, Yanagido 1-1, Gifu 501-1193, Japan
e-mail: ando@gifu-u.ac.jp

K. Morokuma
Fukui Institute for Fundamental Chemistry, Kyoto University,
Takano-Nishihiraki-cho 34-4, Kyoto 606-8103, Japan

K. Morokuma
Cherry L. Emerson Center for Scientific Computation
and Department of Chemistry, Emory University,
Atlanta, GA 30322, USA

showed that the alkylation reaction of lithium enolates occurs via the monomeric ion pair even in the presence of a large excess of tetrameric and dimeric forms including mixed aggregates with LiBr in many examples [7–17]. In fact, the enolate experiment is usually performed at around the 0.1 mol/L concentration, corresponding to the enolate/THF molecular ratio of 1:123. This dilution and the solvation free energy would favor monomeric species unless the dimerization free energy is very large. Therefore, we consider only the monomeric enolate.

Here, we show our theoretical study on the alkylation reaction of the lithium enolate monomer of acetaldehyde with methyl chloride in the presence of 0–6 THF molecule(s). THF is the most common solvent for the alkylation reaction of enolates. In order to estimate the solvent effect, dimethyl ether has been used as coordinating solvent instead of THF in theoretical studies [6, 7, 18–26] except for the structural studies of some lithium compounds [27–31]. Although, dimethyl ether has about the same basicity and steric effect around the ether oxygen as THF, the space which THF molecule takes is sometimes important for the steric environment when reactions occur.[1] In the study on the origin of π-facial stereoselectivity in the alkylation of lithium enolate, one of us used dimethyl ether in order to examine the effect of solvent [18]. The dimethyl ether molecule interacted with both the lithium cation and the leaving chloride anion in some cases, where these interactions caused the transition structures to become unfavorable because of substantial entropy loss. Therefore, in the present study, 1–6 THF molecules were explicitly included in the calculation, intended to solvate the lithium cation and the chloride anion with them. Since reports show that the DFT methods provide reasonable results with relatively lower cost for cluster systems, [6, 18, 32] the calculations were performed using the B3LYP hybrid functional [33, 34] together with the 6–31(+)G* basis set (see Sect. 2).

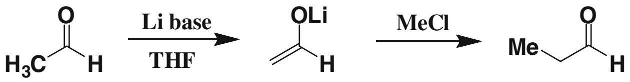

Another aim in this study is to obtain as accurate results as possible for large solvated cluster systems using the two-layer MO + MO version of ONIOM method [35–43]. In this procedure, the molecular system being studied is divided into two layers. The active part of the reaction ("model" system) is treated with both at "high" and "low" levels of MO calculation, whereas the entire "real" system is treated only at the "low" level of MO calculation, and they are integrated to define the ONIOM total energy of the entire system. The ONIOM energy is defined as

$$\mathrm{E(ONIOM)} = \mathrm{E(High,\ model)} + \mathrm{E(Low,\ real)} - \mathrm{E(Low,\ model)}$$

Here, H_2O molecules are used as the high-level model (with two H atoms in H_2O being the link atoms) for the three THF molecules that solvate the lithium cation, and the other atoms in THF are treated only at the low level. Three other THF molecules that solvate the leaving chloride anion are treated only at the low level. We will compare geometries of substrate complexes, transition structures, and products of the reaction optimized at the ONIOM combination (high = B3LYP/6–31(+)G*: low = RHF/3–21 G*) with the results obtained from the B3LYP/6–31(+)G* level.

2 Methods of calculation

All the calculations were performed using the Gaussian 03 program [44]. For the higher levels of calculations, the basis set (denote as 6–31(+)G* [45]) consisting of the 6–31 G* basis set for Li and the 6–31+G* basis set for C, H, O, and Cl was used because of the incompatibility of the PCM calculations with lithium atom with a diffuse function. We believe the diffuse function for the lithium atom is not important at least for the lithium enolate chemistry. Vibrational frequency calculations gave no or only one imaginary frequency for all reactant complexes and transition structures, respectively. The structures of reactants and products were obtained by the optimization from the last structures on both sides of the IRC calculations [46–48]. The harmonic vibrational frequencies were scaled by 0.9409 for the HF/3–21 G* results and unscaled for the B3LYP results [49, 50]. The Gibbs free energies in gas phase were calculated at 298.15 K and 1 atm. ΔE at the B3LYP/6–31(+)G* level reported here are the differences in the sum of electronic and zero-point energies.

The solvation was modeled by microsolvation with THF molecules on both the lithium atom and the leaving chloride atom as well as the polarizable continuum model. The single-point self-consistent reaction field (SCRF) technique for THF ($\varepsilon = 7.58$) is also used with and without the microsolvation with THF in order to examine the bulk solvent effects. Among the SCRF methods, Tomasi's polarized continuum model with the integral equation formalism (IEFPCM) was used in this study [51]. Since the continuum solvent model implemented in Gaussian 03 was incompatible with lithium compounds for optimization, [27] single-point energy calculations were performed for the lithium containing species.

---

[1] Dimethyl ether was reported to be not a satisfactory substitute for THF in predicting the aggregation states of lithium dialkylamides [27].

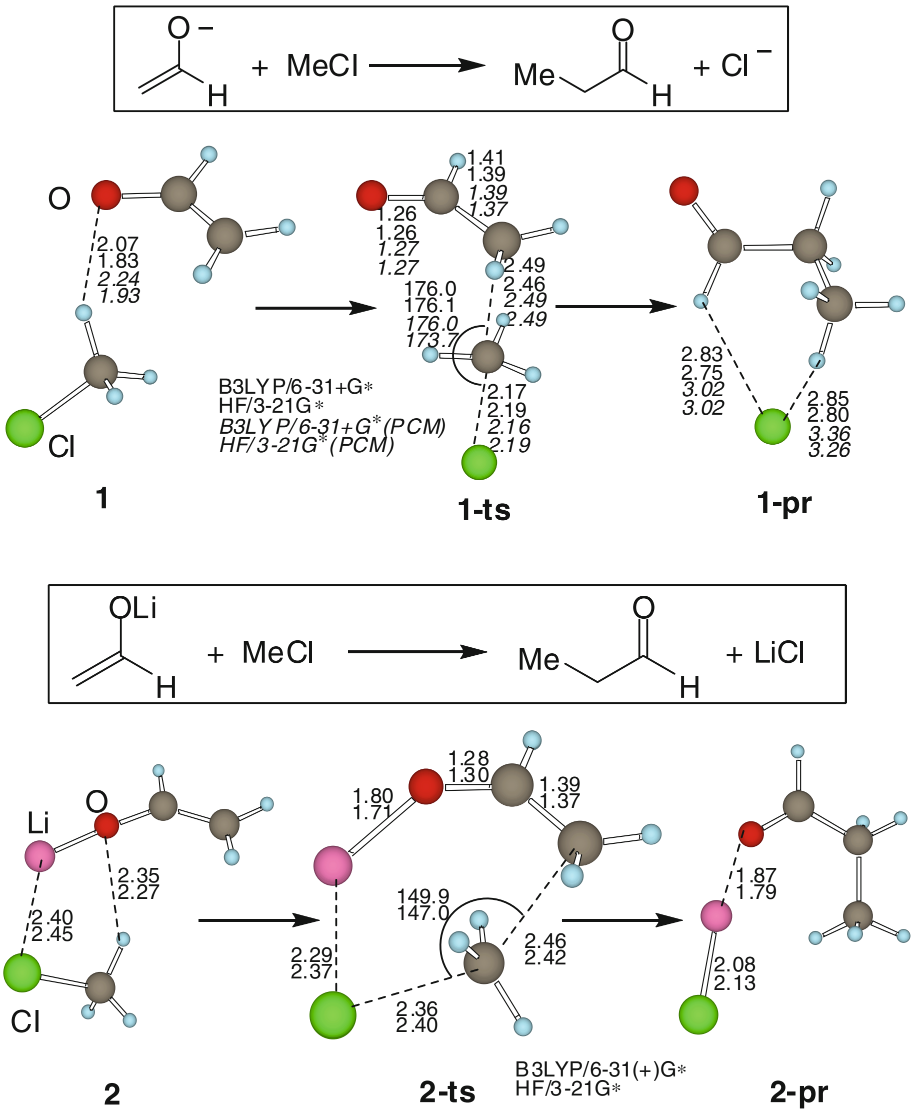

Fig. 1 The transition structures for the alkylation reaction of the acetaldehyde enolates (free enolate **1** and lithium enolate **2**) with methyl chloride. The numbers in the structures are the bond lengths (Å) and bond angles (°) in the level of calculations as shown at their side, respectively

3 Results and discussion

3.1 Free enolate + methyl chloride

The simplest model reaction, the alkylation reaction of the free enolate derived from acetaldehyde with methyl chloride, was studied first (Fig. 1 and Table 1). The transition structure **1-ts** was located at both the B3LYP/6–31+G* and HF/3–21 G* levels. The distances of the forming C–C bond are 2.49 and 2.46 Å, respectively. Although, the activation free energy at the B3LYP level (6.7 kcal/mol) is much lower than that at the HF level by 6.5 kcal/mol, the TS structures are not so different. In order to see the reaction in solution, the transition structures were re-optimized using the SCRF (IEFPCM, solvent = THF) method. The distances of the forming C–C and the breaking C–Cl bond are very similar to the gas-phase values (see the *italic numbers* in Fig. 1) but the activation energies (5.5 and 9.6 kcal/mol) are lower than those of the gas-phase values by 1.2 and 3.6 kcal/mol, respectively (Table 1). Since the single-point energy calculations (PCM (SP)) at the gas phase structures gave almost the same activation energies as those at the PCM-optimized structures (Table 1), only single-point PCM energies were calculated for the other structures.

3.2 Lithium enolate + methyl chloride

The effects of a lithium ion were studied using lithium enolate as the reacting agent. The transition structure **2-ts** for the reaction of the lithium enolate with methyl chloride was located at the B3LYP/6–31 (+) G* level (the bottom of Fig. 1 and Table 2). The distance of the forming C–C bond is 0.03 Å shorter compared to the corresponding **1-ts** structure, and the activation free energy is 21.3 kcal/mol, which is higher than that of **1-ts** by 14.6 kcal/mol in gas phase. Because of the strong interaction between the

Table 1 The relative energies for the reaction of CH_2=CHO^- with MeCl (kcal/mol)

Level	1	1-ts	1-pr
ΔG (B3LYP/6–31+G*)	0	+6.7	−41.2
ΔG (HF/3–21G*)	0	+13.2	−55.0
ΔG (B3LYP/6–31+G*//HF/3–21G*)	0	+4.5	−42.6
ΔE (B3LYP/6–31+G*, PCM)	0	+5.5	−48.8
ΔE (B3LYP/6–31+G*, PCM (SP))	0	+5.4	−49.5
ΔE (HF/3–21G*, PCM)	0	+9.6	−68.3
ΔE (HF/3–21G*, PCM (SP))	0	+9.4	−68.4
ΔE (B3LYP/6–31+G*,PCM (SP)//HF)	0	+5.0	−51.1

Table 2 The relative energies for the reaction of CH_2=CHOLi with MeCl (kcal/mol)

Level	2	2-ts	2-pr
ΔG (B3LYP/6–31(+)G*)	0	+21.3	−43.1
ΔG (HF/3–21G*)	0	+31.0	−48.4
ΔG (B3LYP/6–31(+)G*//HF/3–21G*)	0	+22.3	−44.0
ΔE (B3LYP/6–31(+)G*, PCM (SP))	0	+18.7	−47.0
ΔE (HF/3–21G*, PCM(SP))	0	+23.4	−58.7
ΔE (B3LYP/6–31(+)G*, PCM (SP)//HF)	0	+17.3	−49.4

leaving chlorine atom and the lithium cation in the transition state, the cyclic transition structure is obtained. When the nucleophile donates its electrons to the σ* orbital of the C–X bond in the S_N2 reaction, the ideal angle C–C–Cl is 180°. However, the enolate nucleophile attacks the methyl chloride at C–C–Cl of 149.9° in this cyclic transition structure. Thus, this arrangement caused the transition structure to be less stable by a loss of overlap of the σ* orbital with the nucleophile lone pair and to have a higher activation energy. Similar transition structures were previously reported for the same system by Streitwieser (for a review, see [7]) and Pratt [32]. The PCM energy calculated using the gas phase structure **2-ts** is lower than the gas-phase value by 2.6 kcal/mol (Table 2). Although, this solvation energy is larger than that of **1-ts** (1.3 kcal/mol), the activation energy in solution (18.7 kcal/mol) is much higher than that expected from experimental results (The stereoselective alkylation can be performed at low temperature such as −78 °C). The calculations at the HF/3–21G* level gave a much higher activation energy and not much different structures.

3.3 Lithium enolate + methyl chloride + one THF molecule

Since the alkylation reaction of the lithium enolate is generally performed in THF, solvation of the lithium ion (as well as that of the leaving chloride ion) is expected to be important. Since PCM is not able to account for site-specific interaction between solvent molecules and the reacting species, we have included one THF molecule explicitly into calculation, together with PCM. THF is assumed to coordinate with its ether oxygen to the lithium ion.

Three transition structures for the reaction of the lithium enolate coordinated with one THF molecule with methyl chloride were located as shown in Fig. 2 and Table 3. In the transition structure **3-ts**, the THF molecule participated in the formation of a large cyclic structure involving both MeCl and enolate; THF is coordinated to the lithium cation by its oxygen and also to the leaving chloride by its hydrogen atoms. The angle C–C–Cl at the reaction center is almost linear, 171.8°. Because of the interaction of the THF hydrogens with the leaving chloride, the angle is slightly smaller than 176.0° for **1-ts**. The distance of the forming C–C bond is 2.23 Å (without PCM, as discussed in Sect. 2), 0.26 and 0.23 Å shorter than the corresponding values of **1** and **2-ts**, respectively. TS **3-ts** is stabilized by the strong interaction between Li cation and THF oxygen with the Li···O distance of 1.85 Å as well as the weaker interaction between the leaving chloride anion and the THF hydrogen atoms with the Cl···H distance of ∼2.8 Å. The PCM single-point (SP) activation energy from **3** to **3-ts** is 9.6 kcal/mol and is much lower than in the gas-phase value by 15.5 kcal/mol (Table 3), suggesting that the bulk solvation handled by PCM still has a substantial effect even after one THF molecule is explicitly included. This point will be discussed by including more than one THF molecule in the following section. The activation energy with PCM for **3-ts** (9.6 kcal/mol) is larger than 5.4–5.5 kcal/mol for **1-ts** and substantially smaller than 18.7 kcal/mol for **2-ts**. This clearly confirms that PCM totally misses the local interaction essential for discussion of reactions in strongly coordinating solution. We also found another transition structure, **3-tsA**. Only the conformation of THF is different from and the energy is almost same as that of **3-ts** (see Fig. 2 and Table 3). Thus, we will not discuss **3-tsA** explicitly.

The third transition structure **3-tsB** retains the cyclic structure of **2-ts**, with a strong interaction between the leaving chlorine anion and the lithium cation and with the enolate nucleophile attacking the methyl chloride at 147.7°. The THF molecule is coordinated to the lithium cation with its oxygen atom. Both the structure and the activation energy of **3-tsB** are similar to those of **2-ts**; the THF coordination did not affect much for this cyclic transition structure. The activation energy for **3-tsB** in PCM (17.5 kcal/mol) is much higher than that for **3-ts**, and we can conclude that this cyclic transition structure does not contribute to the reaction in solution.

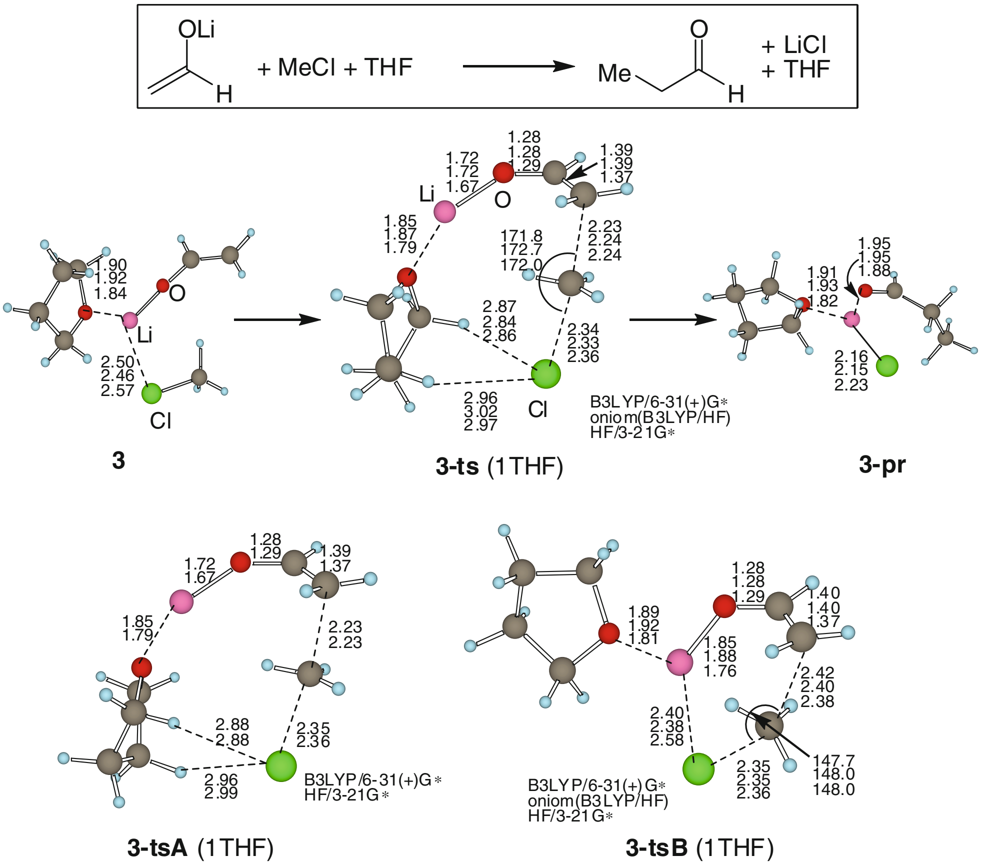

Fig. 2 The transition structures for the alkylation reaction of the acetaldehyde lithium enolates with methyl chloride in the presence of 1 THF. The numbers in the structures are the bond lengths (Å) and bond angles (°) in the level of calculations as shown at their side, respectively

The transition structures **3-ts** and **3-tsB** were also located at the ONIOM combination (high = B3LYP/6–31(+)G*: low = RHF/3–21 G*) where the THF molecule except for the oxygen atom (H_2O in the "model" system) was treated only at the low level. The structures of both **3-ts** and **3-tsB** are almost same as those at the pure QM level (see the bond lengths in Fig. 2). The ONIOM energetics is very similar to the pure QM results in every case with an ONIOM error of less than 1 kcal/mol, suggesting that this ONIOM combination works well for the present system.

3.4 Lithium enolate + methyl chloride + two THF molecules

With two THF molecules for the reaction of the lithium enolate with methyl chloride, **4-ts** was located as the most stable transition state (Fig. 3 and Table 4). The structure **4-ts** has two THF molecules coordinated with their oxygen atoms to the lithium cation and can be considered to be an extended system of the most stable TS structure **3-ts** having one THF molecule, to which the second THF molecule has coordinated at the lithium cation from the open side of **3-ts**. Since two THF molecules donate their electrons to the lithium cation, the enolate O–Li bond length became longer (1.77 Å vs. 1.72 Å in **3-ts**). The C–C–Cl angle (174.3°) is larger than 171.8° in **3-ts** and only slightly smaller than the value for **1-ts** (176°). The distance of the forming C–C bond is 2.24 Å, almost same as that of **3-ts**. The activation free energy in PCM, 9.3 kcal/mol, is slightly smaller than 9.6 kcal/mol in **3-ts**. Additional coordination of the lithium cation by the second THF makes the TS a little earlier and lower in energy.

3.5 Lithium enolate + methyl chloride + 3–6 THF molecules

The transition structures **5–8-ts** for the reaction of the lithium enolate in the presence of 3–6 THF molecules, respectively, with methyl chloride were located (Fig. 3 and Table 4). In the presence of three THF molecules, in **5-ts**, the lithium cation becomes tetrahedrally coordinated by the substrate enolate group and the oxygens of three THF molecules; two of these THF molecules interact also with the leaving chloride by their two hydrogen atoms (2.85 and 2.94 Å). The distances of the forming C–C bond and the cleaving C–Cl bond are 2.28 and 2.30 Å, respectively, and **5-ts** is a little earlier compared with **4-ts** (2.24 and 2.33 Å).

Although, **5-ts** has a tetra-coordinated lithium cation (the lengths of the three Li–O(THF) bonds are 1.98–2.01 Å) and the enolate O–Li bond becomes longer (1.84 Å) than that of

Table 3 The relative energies for the reaction of CH_2=CHOLi with MeCl in the presence of one THF molecule (kcal/mol)

Level	3	3-ts	3-pr
ΔG (B3LYP/6–31(+)G*)	0	+25.1	−40.4
ΔG (oniom (B3LYP: HF))	0	+24.6	−40.4
ΔG (HF/3–21G*)	0	+29.6	−45.1
ΔG (B3LYP/6–31(+)G*//HF/3–21G*)	0	+24.6	−40.7
ΔE (B3LYP/6–31(+)G*, PCM(SP)	0	+9.6	−48.2
ΔE (B3LYP/6–31(+)G*, PCM (SP)//ONIOM)	0	+7.8	−49.5
ΔE (B3LYP/6–31(+)G*, PCM(SP)//HF)	0	+8.7	−49.0
ΔE (HF/3–21G*, PCM (SP))	0	+12.2	−56.8
A			
ΔG (B3LYP/6–31(+)G*	+0.34	+25.4	−39.5
ΔG (HF/3–21G*)	+0.08	+29.8	−45.1
B			
ΔG (B3LYP/6–31(+)G*)	0	+22.3	−38.7
ΔG (ONIOM (B3LYP: HF))	0	+22.2	−39.4
ΔG (HF/3–21 G*)	0	+30.4	−44.6
ΔE (B3LYP/6–31(+)G*, PCM (SP))	0	+17.4	−47.0
ΔE (B3LYP/6–31(+)G*, PCM (SP)//ONIOM)	0	+17.2	−48.5
ΔE (B3LYP/6–31(+)G*, PCM (SP)//HF)	0	+17.3	−48.7
ΔE (HF/3–21 G*, PCM (SP))	0	+23.2	−57.8

4-ts (1.77 Å), the activation free energy at the B3LYP level in gas phase (19.5 kcal/mol) is slightly higher than that of **4-ts** [19.0 kcal/mol] (Table 4). For monodentate ethers, coordination is accompanied by substantial loss of entropy [6, 18, 19], and it is experimentally known that lithium sometimes does not reach tetra-coordination with external ligands especially in sterically crowded environment [52–54]. In fact, both ΔE corrected for ZPE in gas phase and the PCM energy of **5-ts** are lower than that of **4-ts** by 0.7 kcal/mol.

In the presence of four THF molecules, in **6-ts,** the lithium cation remains tetra-coordinated by the enolate O and oxygens of three THF molecules, as in **5-ts**. The fourth THF molecule interacts with the leaving chloride anion by two of its hydrogen atoms as well as with a hydrogen atom of another THF with the oxygen atom. The essential tetra-coordination of lithium cation is completed by three THF molecules in **5-ts**, and the fourth THF molecule in **6-ts** can be considered as a "solvent molecule" not participating in the stabilization of the Li reaction center. The leaving chloride is stabilized by the interaction with four hydrogen atoms of three THF molecules (2.83–3.14 Å) in **6-ts**. Although **6-ts** (2.30 Å) is slightly later than **5-ts** (2.28 Å), both the enolate structure and the distances of three Li–O(THF) bonds in **5** and **6-ts** are almost same. Because of the extra interaction at the chloride center, the activation free energy in gas phase (18.1 kcal/mol) is lower than that of **5-ts** (where two hydrogen atoms interacted with the chloride) by 1.4 kcal/mol. The activation free energy in PCM is 9.0 kcal/mol and is slightly higher than that of **5-ts** (8.6 kcal/mol); the bulk solvation effect is less important in **6-ts**, where one more THF is explicitly included.

In the presence of 5 or 6 THF molecules, the tetra-coordination structure of the lithium cation is essentially unchanged from the case of **5-ts**. The fifth THF molecule is coordinated to the chloride and hydrogen-bonded to the fourth THF molecule, and the sixth THF molecule also is coordinated to the chloride and hydrogen-bonded to the fifth THF molecule. Although the leaving chloride anion was stabilized by the interaction with four hydrogens of three THF molecules in **7-ts** and four THF molecules in **8-ts**, the Cl···H distances are 2.91–3.26 and 2.96–3.12 Å, respectively, and slightly longer than those of **6-ts** (2.83–3.14 Å). The distances of the forming C–C bond are 2.31 and 2.30 Å, and the structures of **7-** and **8-ts** are almost same as that of **6-ts**. The activation free energies of both **7-** and **8-ts** are 16.4 and 17.0 kcal/mol in gas phase, which are lower than **6-ts** by 1.7 and 1.1 kcal/mol, respectively, presumably due to these extra coordinations of the leaving chloride. The activation energies in PCM are 10.3 kcal/mol in **7-ts** and 10.9 kcal/mol in **8-ts**, and larger than that of **6-ts** (9.0 kcal/mol). It appears that the stronger solvation by polarizable continuum in **6-ts** is surpassing the microsolvation plus a weaker (with larger radius) continuum solvation in **7-** and **8-ts**. Although ideally the microsolvation plus continuum calculations should converge to a certain limit as the microsolvation shell expands, obviously the convergence is not reached in the present case.

Fig. 3 The transition structures for the alkylation reaction of the acetaldehyde lithium enolates with methyl chloride in the presence of 2–6 THF molecules at the B3LYP/6–31+G*, the ONIM (B3LYP/6–31+G*: HF/3–21 G*), and the HF/3–21 G* levels. The numbers in the structures are the bond lengths (Å) and bond angles (°)

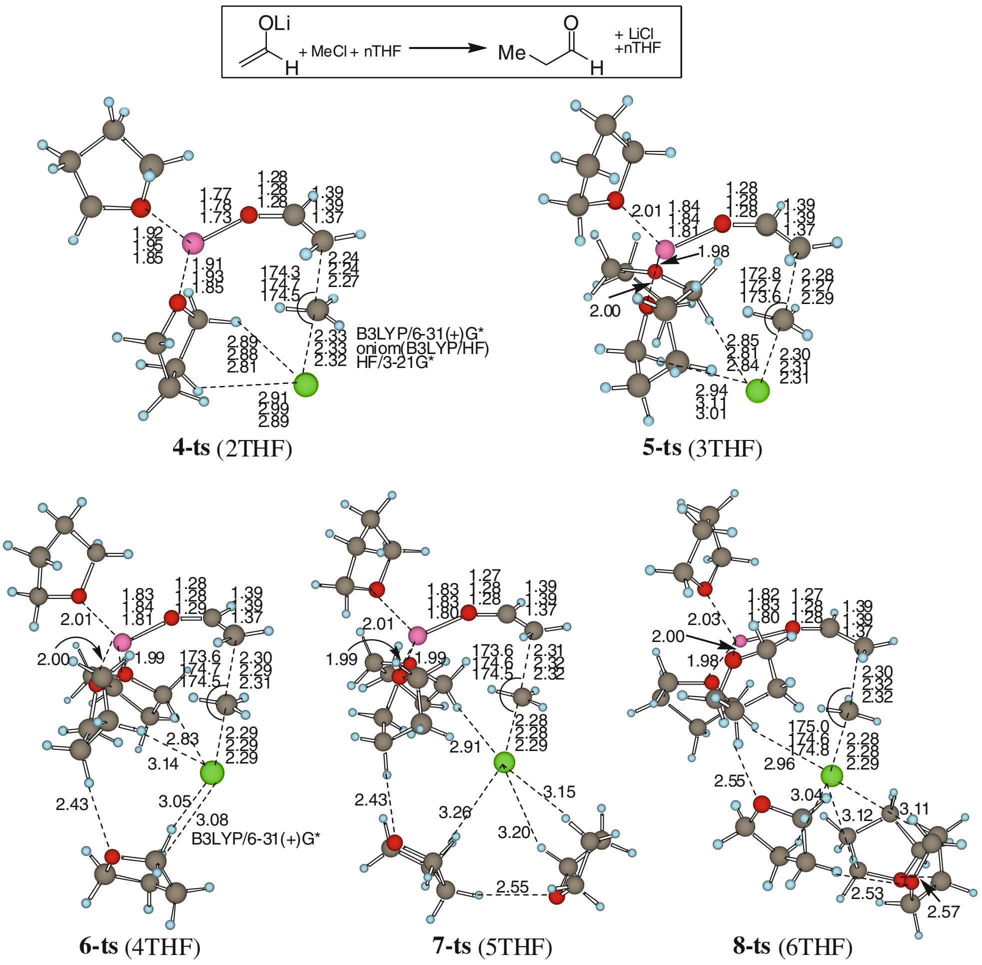

4-ts (2THF) **5-ts** (3THF)

6-ts (4THF) **7-ts** (5THF) **8-ts** (6THF)

Table 4 The relative energies of transition state **2-** to **8-ts** (relative to the reactant complex) of the reaction of CH_2=CHOLi with MeCl in the presence of 0–6 THF molecules (kcal/mol)

Level	2-ts	3-ts	4-ts	5-ts	6-ts	7-ts	8-ts
ΔG (B3LYP/6–31(+)G*)	21.3	25.1	19.0	19.5	18.1	16.4	17.0
ΔE (B3LYP/6–31(+)G*)	18.6	22.3	16.9	16.2	14.8	14.4	13.2
ΔG (ONIOM (B3LYP: HF))	–	24.6	19.1	19.3	16.4	16.0	16.0
ΔG (B3LYP/6–31(+)G*, PCM (SP))	18.7	9.6	9.3	8.6	9.0	10.3	10.9

3.6 Overall reaction mechanism in THF solution

For discussion of the overall reaction mechanism, the energy profiles (ΔE with ZPE in gas phase, ΔG in gas phase, and ΔE in solution corrected with gas phase ZPE and single-point PCM solvation free energy in THF) for reactant complexes and TSs of the reaction of the enolate–MeCl for $n = 0$–6, THF molecules are compared with the reference (the reactant complex **2** + n (THF)) in Table 5, and ΔE in THF is illustrated in Fig. 4, all at the B3LYP/6–31(+)G* level.

If one considers the present reaction in gas-phase clusters, ΔG in gas phase would be a good measure of energy. Here, the reactant complex **3** with one THF molecule is the most stable reactant complex among all n's, while two THF molecules give the most favorable transition state **4-ts**. This can be seen compared with ΔE corrected for ZPE in gas phase; the latter gives the most preferred reactant complexes for **5** and **6** and transition state for **5-** and **6-ts**. The entropic effect in gas phase shifts the most preferred structures to smaller n; aligning the solvent molecules costs entropic energy.

In solution, the gas-phase entropic effect mainly coming from the relative translation and rotation of the components is quenched, as components are individually solvated and the solvation free energy has been taken care of by the

Table 5 The relative energies of the reactant complexes and TSs based on [**2** + *n* (THF)] in the presence of 0–6 THF molecule(s) (kcal/mol) at the B3LYP/6–31(+)G* level

Number of THF Reactant complex	$n = 0$ **2**	$n = 1$ **3**	$n = 2$ **4**	$n = 3$ **5**	$n = 4$ **6**	$n = 5$ **7**	$n = 6$ **8**
ΔE	0.0	−16.3	−24.2	−29.9	−28.6	−27.5	−25.3
ΔG	0.0	−6.4	−3.7	2.0	12.8	23.7	34.1
ΔE (PCM (SP))	0.0	−0.3	−3.0	−3.9	3.0	10.4	18.4
Transition state	**2-ts**	**3-ts**	**4-ts**	**5-ts**	**6-ts**	**7-ts**	**8-ts**
ΔE	18.6	6.1	−7.3	−13.7	−13.9	−13.1	−12.1
ΔG	21.3	18.7	15.3	21.5	30.9	40.1	51.2
ΔE (PCM (SP))	18.7	9.3	6.4	4.6	12.0	20.7	29.3

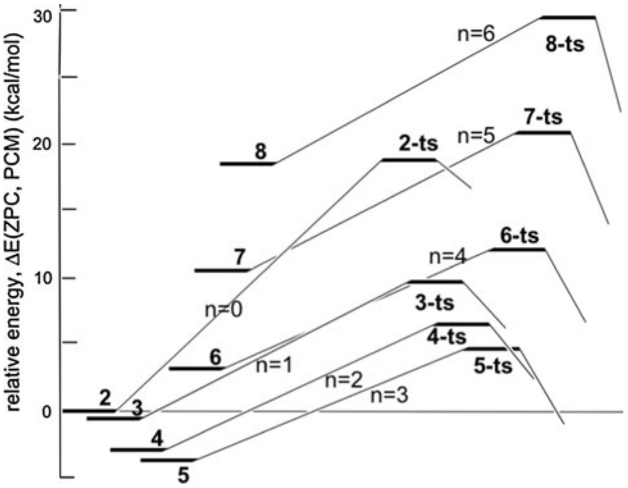

Fig. 4 The energies in solution (ΔE with ZPE and single-point PCM corrections for THF) of the reactant complexes and TSs for the reaction of CH_2=CHOLi with MeCl in the presence of 0 to 6 (*n*) THF molecules based on [**2** + *n* (THF)] (in kcal/mol) at the B3LYP/6–31(+)G* level

PCM calculation. Therefore, we compare ΔE (B3LYP/6–31 (+) G*,PCM (SP)) with gas phase ZPE correction. The results in Fig. 4 show that the activation barrier in solution, measured as ΔE (**n-ts**) – ΔE (**n**) becomes minimum at $n = 3$, with $n = 4$ following slightly behind. Furthermore, when the reactant complex is compared among different n, the complex **5** ($n = 3$) including three explicit THF molecules ($n = 3$) is the lowest in energy and is the most preferred species in solution. The same applies for the transition state; **ts-5** ($n = 3$) is the lowest transition state among different n's. The preference of larger cluster structures in solution compared to the gas-phase cluster originates mainly from the entropic effect. The order of ΔE (ZPE) in solution is not much different from that in gas phase.

The computational results suggest that the site-specific complex with three THF molecules provides the lowest energy and dominant pathway in solution from the reactant complex to the transition state. As discussed above, this pathway involves the direct involvement of two THF molecules in the bridging interaction between Li^+ and Cl^- and one additional THF molecule strongly coordinating Li^+. These specific interactions are essential for the stability of this pathway, which cannot be accounted for by a PCM calculation. The complexes with two or less explicitly considered THF molecules are higher in energy because the specific solvation shell is not completed. The complexes with four or more explicit THF molecules are higher in energy, because the coordination shell for the Li cation is already full and additional THF molecules do not provide strong site-specific interaction.

In summary, the reaction of free enolate anion with MeCl has an early transition state **1-ts** with low barrier (6.7 kcal/mol). The reaction of neutral lithium enolate with MeCl has a cyclic transition structure **2-ts,** and the activation energy was increased to 21.3 kcal/mol. Neither of these models resembles what is found with explicit THF molecules.

In the presence of one THF molecule, in the most stable **3-ts,** the THF molecule, lithium enolate, and methyl chloride form a cyclic structure; **3-ts** has a typical S_N2 transition structure, stabilized by the interaction of a THF molecule with both the lithium cation and the leaving chloride. Although, in **3-ts,** the gas phase activation energy is high (25.1 kcal/mol), the PCM bulk solvation lowers the barrier to 9.6 kcal/mol, almost as low as those of larger models. The second and third THF molecules coordinate with the lithium cation and stabilize the gas phase TS energies further in **4-** and **5-ts**. The tetra-coordination of lithium is completed at **5-ts**. The fourth, fifth, and sixth THF molecules in **6-**, **7-** and **8-ts**, respectively, coordinate the leaving chloride together with some extra week hydrogen bonds with other THF molecules. The activation energy in gas phase decreases dramatically up to **4-ts**, after which it continue to decrease by 0.5–1.7 kcal/mol per THF molecule up to **7-ts**. The activation energy in PCM decreases very slowly from 9.6 kcal/mol in **3-ts** to

8.6 kcal/mol in **5-ts** and increases gradually to 10.9 kcal/mol in **8-ts**.

The present results suggest that **3-ts**, the model with one explicit THF molecule, at least very qualitatively give reasonable TS geometries and PCM activation energies and can be a simplest model for the reaction. On the other hand, the model with three THF molecules, **5-ts**, describes the tetra-coordination of the lithium cation and can be considered to be an optimal model for the present reaction in solution.

The transition structures for the reaction of the lithium enolate with MeCl in the presence of one to six THF molecules were also located at the ONIOM level (B3LYP/6–31 + G*: HF/3–21 G*). All the structures and the activation energies are almost same as the results at the B3LYP level.

Acknowledgments Kaori Ando thanks the Emerson Fellowship for 2-month stay at Emory University. Authors acknowledge the Research Center for Computational Science, Institute for Molecular Science, Okazaki, Japan, for the use of VPP5000 and SX7 computers.

References

1. Seebach D (1988) Angew Chem Int Ed Engl 27:1624–1654
2. Ando K, Green NS, Li Y, Houk KN (1999) J Am Chem Soc 121:5334–5335
3. Meyers AI, Seefeld MA, Lefker BA, Blake JF, Williared PG (1998) J Am Chem Soc 120:7429–7438
4. Ohno H, Ando K, Hamaguchi H, Takeda Y, Tanaka T (2002) J Am Chem Soc 124:15255–15266
5. Tomioka K, Ando K, Takemasa Y, Koga K (1984) J Am Chem Soc 106:2718–2719
6. Abbotto A, Streitwieser A, Schleyer PVR (1997) J Am Chem Soc 119:11255–11268
7. Streitwieser A (2006) J Mol Model 12:673–680
8. Abu-Hasanayn F, Stratakis M, Streitwieser A (1995) J Org Chem 60:4688–4689
9. Abbotto A, Streitwieser A (1995) J Am Chem Soc 117:6358–6359
10. Abu-Hasanayn F, Streitwieser A (1996) J Am Chem Soc 118:8136–8137
11. Abbotto A, Leung SS-W, Streitwieser A, Kilway KV (1998) J Am Chem Soc 120:10807–10813
12. Wang DZ, Kim Y-J, Streitwieser A (2000) J Am Chem Soc 122:10754–10760
13. Streitwieser A, Juaristi E, Kim Y-J, Pugh JK (2000) Org Lett 2:3739–3741
14. Streitwieser A, Kim Y-J, Wang DZ-R (2001) Org Lett 3:2599–2601
15. Kim Y-J, Streitwieser A (2002) Org Lett 4:573–575
16. Wang DZ, Streitwieser A (2003) J Org Chem 68:8936–8942
17. Ando K (2006) J Org Chem 71:1837–1850
18. Ando K (2005) J Am Chem Soc 127:3964–3972
19. Ando K (1999) J Org Chem 64:6815–6821
20. More MB, Glendening ED, Ray D, Feller D, Armentrout PB (1996) J Phys Chem 100:1605–1614
21. Pratt LM, Ramachandran B, Xidos JD, Cramer CJ, Truhlar DG (2002) J Org Chem 67:7607–7612
22. Brandt P, Haeffner F (2003) J Am Chem Soc 125:48–49
23. Parisel O, Fressigne C, Maddaluno J, Giessner-Prettre C (2003) J Org Chem 68:1290–1294
24. Pratt LM, Streitwieser A (2003) J Org Chem 68:2830–2838
25. Pratt LM, Mogali S, Glinton K (2003) J Org Chem 68:6484–6488
26. Streitwieser A, Jayasree EG (2007) J Org Chem 72:1785–1798
27. Pratt LM (2005) Bull Chem Soc Jpn 78:890–898
28. Pratt LM, Nguyen NV, Le LT (2005) J Org Chem 78:2294–2298
29. Pratt LM, Truhlar DG, Cramer CJ, Kass SR, Thompson JD, Xidos JD (2007) J Org Chem 72:2962
30. De Vries TS, Goswami A, Liou LR, Gruver JM, Jayne E, Collum DB (2009) J Am Chem Soc 131:13142–13154
31. Viciu MS, Gupta L, Collum DB (2010) J Am Chem Soc 132:6361–6365
32. Pratt LM, Nguyen NV, Ramachandran B (2005) J Org Chem 70:4279–4283
33. Becke AD (1993) J Chem Phys 98:5648–5652
34. Lee C, Yang W, Parr RG (1988) Phys Rev B 37:785–789
35. Maseras F, Morokuma K (1995) J Comput Chem 16:1170–1179
36. Svensson M, Humbel S, Froese RD, Matsubara T, Sieber S, Morokuma K (1996) J Phys Chem 100:19357–19363
37. Humbel S, Sieber S, Morokuma K (1996) J Chem Phys 105:1959–1967
38. Svensson M, Humbel S, Morokuma K (1996) J Chem Phys 105:3654–3661
39. Vreven T, Morokuma K (2000) J Comput Chem 21:1419–1432
40. Re S, Morokuma K (2001) J Phys Chem A 105:7185–7197
41. Vreven T, Mennucci B, Silva CO, Morokuma K, Tomasi J (2001) J Chem Phys 115:62–72
42. Fukaya H, Morokuma K (2003) J Org Chem 68:8170–8178
43. Mo SJ, Vreven T, Mennucci B, Morokuma K, Tomasi J (2004) Theor Chem Acc 111:154–161
44. Frisch MJ, Trucks GW, Schlegel HB, Scuseria GE, Robb MA, Cheeseman JR, Montgomery JA Jr, Vreven T, Kudin KN, Burant JC, Millam JM, Iyengar SS, Tomasi J, Barone V, Mennucci M, Cossi M, Scalmani G, Rega N, Petersson GA, Nakatsuji H, Hada M, Ehara M, Toyota K, Fukuda R, Hasegawa J, Ishida M, Nakajima T, Honda Y, Kitao O, Nakai H, Klene M, Li X, Knox JE, Hratchian HP, Cross JB, Adamo C, Jaramillo J, Gomperts R, Stratmann RE, Yazyev O, Austin AJ, Cammi R, Pomelli C, Ochterski JW, Ayala PY, Morokuma K, Voth GA, Salvador P, Dannenberg JJ, Zakrezwski VG, Dapprich S, Daniels AD, Strain MC, Farkas O, Malick DK, Rabuck AD, Raghavachari K, Foresman JB, Ortiz JV, Cui Q, Baboul AG, Clifford S, Cioslowski J, Stefanov BB, Liu G, Liashenko A, Piskorz P, Komaromi I, Martin RL, Fox DJ, Keith T, Al-Laham MA, Peng CY, Nanayakkara A, Challacombe M, Gill PMW, Johnson B, Chen W, Wong MW, Gonzalez C, Pople JA (2003) Gaussian 03 revision C02. Gaussian, Pittsburgh
45. Satoh T, Ogino Y, Ando K (2005) Tetrahedron 61:10262–10276
46. Fukui K (1981) Acc Chem Res 14:363–368
47. Gonzalez C, Schlegel HB (1989) J Chem Phys 90:2154–2161
48. Gonzalez C, Schlegel HB (1990) J Chem Phys 94:5523–5527
49. Bauschlicher CW Jr, Partridge H (1995) J Chem Phys 103:1788–1791
50. Scott AP, Radom L (1996) J Phys Chem 100:16502–16513
51. Tomasi J, Mennucci B, Cances E (1999) J Mol Struct (Theochem) 464:211–226
52. Jackman LM, Lange BC (1977) Tetrahedron 33:2737–2769
53. Luch BL, Collum DB (1994) J Am Chem Soc 116:6009–6010
54. Hitchcock PB, Lappert MF, Layh M (1999) Angew Chem Int Ed Engl 38:501–504